

Resonant behaviour in double charge exchange reaction of π^+ -mesons on the nuclear photoemulsion

Yu.A. Batusov^{1,a}, T.D. Blokhintseva^{1,b}, G.B. Pontecorvo^{1,2,4,c}, F. Balestra^{2,d}, M.P. Busa^{2,e}, G. Piragino^{2,4,f}, and M.G. Schepkin^{3,g}

¹ Joint Institute for Nuclear Research Dubna, Moscow region, 141980, Russia

² Dipartimento di Fisica Generale “A. Avogadro” Università di Torino and INFN Sezione di Torino, I-10125 Torino, Italy

³ A.I. Alikhanov Institute of Theoretical and Experimental Physics, Moscow, 117218, Russia

⁴ Centro Studi e Ricerche “Enrico Fermi”, Roma, Italy

Received: 10 January 2006 / Revised version: 20 March 2006 /

Published online: 10 May 2006 – © Società Italiana di Fisica / Springer-Verlag 2006

Communicated by M. Garçon

Abstract. The invariant-mass spectra of the $pp\pi^-$ and pp systems produced in the double charge exchange (DCX) of positively charged pions on photoemulsion are analysed. A pronounced peak is observed in the $pp\pi^-$ invariant-mass spectrum, while the M_{pp} spectrum exhibits a strong Migdal-Watson effect of the proton-proton final-state interaction. These findings are in favor of the NN -decoupled $NN\pi$ pseudoscalar resonance with $T = 0$ called d' .

PACS. 13.75.Gx Pion-baryon interactions – 25.80.Hp Pion-induced reactions – 14.20.Pt Dibaryons

1 Introduction

In this paper the spectrum of invariant masses of the $pp\pi^-$ system produced in double charge exchange (DCX) reactions of π^+ -mesons on the nuclei ^{107}Ag and ^{109}Ag in photoemulsion is analysed; a peak has been revealed at $M_{pp\pi^-} \approx 2.05$ GeV. We consider this result as a confirmation of the existence of d' , that was proposed in order to explain the maxima exhibited by the forward-angle DCX cross-section $\pi^+(A, Z) \rightarrow (A, Z + 2)\pi^-$ at $T_{\pi^+} \sim 50$ MeV [1–3]. The energy of the incident π^+ -mesons in the photoemulsion experiment was quite low: $T_{\pi^+} = 40$ –140 MeV, while the resolution in the invariant mass $M_{pp\pi^-}$ amounted to about 10 MeV. Thus, the experimental results may serve as a critical test of the d' -resonance hypothesis. It will be shown that an explanation of the results obtained, based on traditional approaches, does not provide for the reproduction of the maximum in the $M_{pp\pi^-}$ spectrum, which is observed to be precisely in the region occupied by the mass of the resonance and explains the sharp peaks in the DCX re-

actions $\pi^+(A, Z) \rightarrow (A, Z + 2)\pi^-$ on the isotopes ^7Li , $^{12,14}\text{C}$, $^{16,18}\text{O}$, $^{40,42,44,48}\text{Ca}$, ^{56}Fe and ^{93}Nb [1–3].

In sect. 2 of the paper a description of the actual photoemulsion experiment is presented. Section 3 presents the results of previous attempts at searching for d' together with arguments in favour and against the hypothesis. Then, sect. 4 contains a discussion of possible explanations, based on non-resonant mechanisms, of the effects observed. Section 5 provides a comparison of calculations accounting for the resonance with the experimental results. Section 6 contains the conclusions.

2 Experimental procedure

The DCX of π^\pm -mesons was first observed in studies of pion interactions with nuclei of photoemulsion [4–9]. These experiments made use of photomulsion chambers, composed of NIKFI-BR layers 400 and 600 μm thick, that were exposed to π^+ and π^- beams of the phasotron of the JINR Dzhelapov Laboratory of Nuclear Problems; the momentum spread of the pions in the beams was $\sim 3\%$. The dimensions of these photoemulsion chambers were chosen so as to provide for 50–140 MeV π^- -mesons being completely stopped in the emulsion.

The “area” method was applied in searching for stopped π -mesons in the layers of developed emulsion: π^+ -mesons were revealed by the characteristic image of the

^a e-mail: yuabat@nusun.jinr.ru

^b e-mail: blokhin@nusun.jinr.ru

^c e-mail: gilpont@nusun.jinr.ru

^d e-mail: balestra@to.infn.it

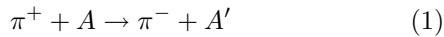
^e e-mail: busa@to.infn.it

^f e-mail: piragino@to.infn.it

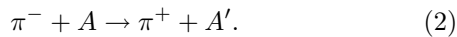
^g e-mail: schepkin@itep.ru

$\pi^+ \rightarrow \mu^+ + \nu_\mu$ decay, while π^- -mesons were recognized by the “ σ -stars”. DCX events in chambers exposed to π^+ -mesons were identified by stops of π^- -mesons, and in chambers exposed to π^- -mesons such events were identified by the decays of π^+ -mesons. The tracks of the stopped mesons were, then, traced back in the emulsion chamber up to their departure from stars formed in the emulsion. Only such nuclear breakup events were chosen for further analysis, in which

- 1) The incident-pion track was present.
- 2) The angle between the incident-pion track and the beam direction did not exceed $\pm 3^\circ$.
- 3) The density of grains along the incident-pion track did not differ (within 10%) from the average density of grains along tracks of the beam particles. Such an analysis of seven photoemulsion chambers (with account of their geometrical registration efficiency) permitted to single out 793 events of the DCX reaction



and 493 events of the reaction¹

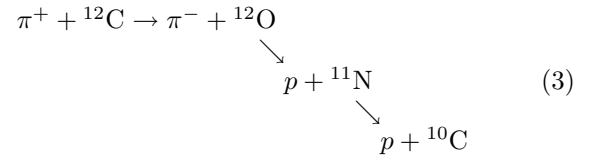


Further analysis of the registered events of π -meson DCX on the nuclei of the photoemulsion [4–9] at initial energies between 40 and 140 MeV permitted to obtain the following characteristics of the processes studied.

1. The cross-section of π^+ -meson DCX exceeds the cross-section of π^- -meson DCX within the entire range of energies studied. If one considers DCX reactions to be the result of pions interacting with separate nucleons or clusters of nucleons in the nucleus, then the said difference may be attributed to several reasons: a) the excess of neutrons in the heavy nuclei (Ag, Br) present in the photoemulsion results in the probability of DCX being higher for π^+ -mesons, than for π^- -mesons. Moreover, additional investigation of the dependence of the DCX cross-section for both π^+ - and π^- -mesons upon the mass of the target nucleus [6] reveals that it increases with the atomic number of the nucleus; consequently, in photoemulsion this process will preferentially proceed on heavy nuclei; b) the emission of secondary π^+ -mesons is hindered by the Coulomb barrier of the nucleus. This imposes additional restrictions on the DCX of π^- -mesons.

2. If all possible reactions of positive π -meson DCX on the nuclei present in the photoemulsion are considered, then it can be verified that stars with one or no prongs cannot be produced on the light nuclei (C, N, O), and, consequently, they result from the interaction of π^+ -mesons with Ag or Br nuclei. The same conclusion can be made concerning two-prong events without an electron at the center of the star [7]. Consider, for example, the reaction

on C nucleus:



with the subsequent beta decay ${}^{10}\text{C} \rightarrow e^+ + \nu_e + {}^{10}\text{B}$.

Such a process in photoemulsion looks either like a three-prong star, or like a two-prong star (when the energy of the residual nucleus ${}^{10}\text{B}$ is low, and it leaves no track in the photoemulsion) with a fast electron track departing from the center of the star.

Similar reactions take place on N and O nuclei.

3. In the case of π^+ -meson DCX two neutrons of the target nucleus are transformed into two protons that can leave the nucleus. This fact is confirmed by the multiplicity distribution of prongs in a star in the case of the registered events of π^+ -meson DCX in photoemulsion. In this case, the average number of charged particles (without account of the secondary π^- -meson and electrons) per “star” for energies ranging from 40 to 140 MeV amounts to 2.07 ± 0.09 . With account of the restrictions obtained it was possible to identify two-prong π^+ -meson events of DCX on the heavy nuclei of the photoemulsion, the percentage of which amounts to $\sim 20\%$. This result was somewhat unexpected, since the Coulomb barrier for Ag and Br nuclei is about 13 MeV, which should significantly hinder the departure of two slow secondary protons.

One may assume that DCX of π^+ -mesons proceeds on a pair of correlated neutrons. Then, a noticeable contribution to the reaction should be due to the $NN\pi$ -resonance, d' .

In order to test this mechanism experimentally, 224 events of π^+ -meson DCX were selected, in which only two protons and a π^- -meson were found in the final state, while no visible tracks of the recoil nucleus or of a fast electron were present at the center of the star.

For each of these selected events, the angles were measured between all secondary charged particles and the incident π -meson track, and the momenta and energies of the particles were determined from their path ranges. The results of these measurements permitted to determine the spectrum of $pp\pi^-$ invariant masses (see sect. 4). Before initiating a detailed discussion of the resonant mechanism of DCX on heavy nuclei, we shall present a short review of earlier experimental searches for the d' -resonance and, also, describe its main properties. For the explanation of DCX on Ag and Br, based on a resonance mechanism, the importance of the existence in the surface layer of the nuclei of a di-neutron should also be noted, which in nuclei with excess neutrons has been confirmed experimentally [9].

¹ These events will not be further discussed, since they cannot be used for the purposes of this paper.

3 Searches for the d' -resonance in strong and electromagnetic processes. Properties of the d' -resonance

As was already mentioned, the d' -resonance was proposed for the explanation of the resonance-like behaviour of the π^+ -meson DCX cross-section at a forward angle for incident-pion energies in the vicinity of $T_{\pi^+} \sim 50$ MeV, which turned out to be unexpected from the point of view of conventional nuclear models (see, for example, ref. [10] and references in ref. [1]). The reactions are DCX $\pi^+(A, Z) \rightarrow (A, Z+2)\pi^-$, in which the final-state nucleus is found either in the ground state (GS) or in the double analog isobaric state (DIAS). Thus, it is reasonable to assume (which is further done in all papers concerning the DCX) the reaction to take place in the outer shells of the nuclei. The idea of DCX as a two-step process resulted in the prediction of minima in the region of $T_{\pi^+} \sim 50$ MeV. This is due to the differential single charge exchange cross-section in this energy region exhibiting deep minima, caused by the destructive interference of s - and p -waves (see review [11]). Contrary to expectations, the first experimental studies of DCX revealed quite clear maxima corresponding to a cross-section exceeding the theoretical predictions [10] by two orders of magnitude. Subsequent experiments (see [12] and references therein), especially devoted to the investigation of DCX in the region of $T_{\pi^+} = 20$ –100 MeV, confirmed the presence of sharp peaks at the same energy, *i.e.* at $T_{\pi^+} \approx 50$ MeV. Of particular interest is DCX on nuclei with doubly closed shells, ^{16}O and ^{40}Ca , for which the DCX cross-section, according to conventional approaches, should be strongly suppressed as compared to DCX on other isotopes (below, the example is presented of the forward-angle DCX cross-section for ^{40}Ca from ref. [13]). But experiments have demonstrated that the DCX cross-sections on all isotopes are of the same order of magnitude. The $NN\pi$ -resonance d' with quantum numbers $J^P = 0^-$, $T = 0$ and mass $M \approx 2m_N + m_\pi + 50$ MeV ≈ 2.06 GeV is ideal for explaining the DCX peaks. Such quantum numbers forbid the decay of d' into a pair of nucleons via strong interaction, so the sole decay channel is the decay into $NN\pi$ ($pp\pi^-$, $nn\pi^+$ and $pn\pi^0$). Here, all the three particles in the final state are in the s -wave with respect to each other². The absence of a 2-particle decay via strong interaction signifies that the decay width into $NN\pi$ with an energy release ~ 50 MeV should be small. Additional suppression of the $d' \rightarrow NN\pi$ decay probability is again due to the absence of the d' coupling to the NN -channel: among the diagrams of the $d' \rightarrow NN\pi$ decay, there are none, in which the π -meson is emitted from the external hadron line. Hence, from the Adler theorem it follows that the 3-particle decay amplitude is proportional to the 4-momentum of the pion. In the case of an s -wave decay involving a small energy release, this signifies that the amplitude contains an additional smallness of the order of m_π/m_N . From the above, the diagram describing

² The electromagnetic decay $d' \rightarrow d\gamma$ is also permitted and it will be dealt with below.

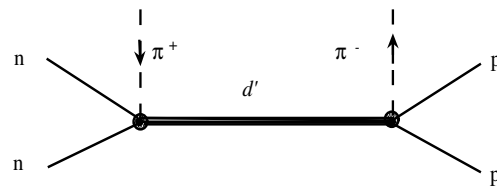


Fig. 1. Diagram of a DCX reaction.

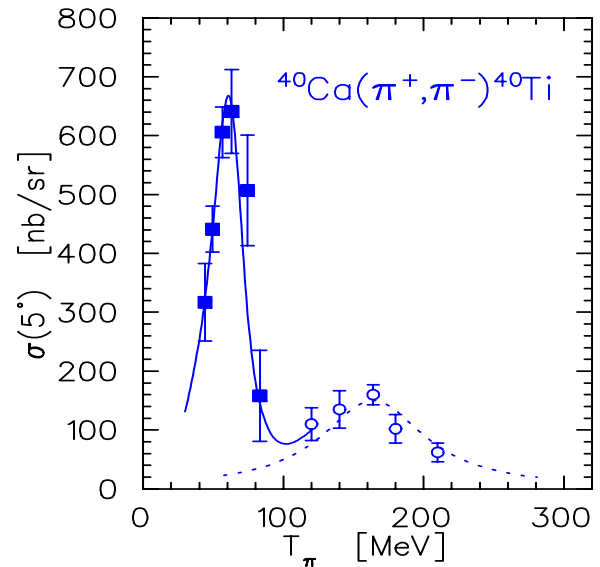


Fig. 2. Energy dependence of the forward-angle DCX cross-section on ^{40}Ca . The full squares represent experimental measurements from ref. [13]. The solid curve shows the d' contribution. The data at $T_\pi \geq 100$ MeV (open circles) are from LAMPF [15,16]. The dotted line represents parametrization of the $\Delta\Delta$ process (for more details see refs. [13,12]).

the contribution of the d' to the pionic DCX is of the form presented in fig. 1.

For a resonance description of DCX, two other parameters were introduced besides the d' mass: the $d'NN\pi$ coupling constant and the d' decay width in a nuclear medium (both the mass and the resonance width in a nuclear medium may differ from their vacuum values). As to the d' width in a nuclear medium, owing to the reaction $d'N \rightarrow 3N$, involving an energy release of 190 MeV, it must exceed the $d' \rightarrow NN\pi$ decay width in vacuum by an order of magnitude [14]. The results of fitting the parameters of the resonance over the entire set of data on DCX [1] are in agreement with calculations based on the aforementioned assumptions [12,14]. The cross-section of the reaction $\pi^+ {}^{40}\text{Ca} \rightarrow {}^{40}\text{Ti} \pi^-$ is presented in fig. 2 as an example of the DCX cross-section behaviour at low energies.

Later, attempts were made [17,18] to explain the peaks qualitatively by nuclear medium effects, but no explanation based on conventional nuclear physics exists, however, for the whole set of data on DCX, and, in particular,

for nuclei with $N = Z$. A series of experiments in search of the d' has been performed at JINR [19,20] and at TRIUMF [21,22], where the DCX $\pi^+ + {}^4\text{He} \rightarrow pppp \pi^-$ was measured. Unlike previous experiments, DCX on ${}^4\text{He}$ results in the production of four protons in the continuum. Therefore, in this reaction the d' production is a threshold phenomenon at an initial energy ~ 80 MeV: 80 MeV = the resonance energy in DCX (50 MeV) plus the binding energy of ${}^4\text{He}$. Besides, the influence of nuclear medium effects on the π -mesons is minimal; one must, however, take into account inelastic interactions of d' with nucleons in the final state [14]. Taking into account such final-state interactions (like in DCX transitions to discrete levels) should result in a significant (approximately by an order of magnitude) decrease in the output of “charge-exchanged” π -mesons, produced via the resonance. Thus, the contribution of the resonance to the DCX turns out to be much reduced: of, say, 100 produced resonances only a few will decay “freely”, like in vacuum, $d' \rightarrow NN\pi$, while the remainder will undergo inelastic collisions with the spectator nucleons: $d'N \rightarrow 3N$. This hinders searches of d' and may explain [14] the absence of a threshold effect in DCX on ${}^3\text{He}$, which was also studied [23] experimentally at TRIUMF, after ${}^4\text{He}$. However, the total cross-section for ${}^4\text{He}$ as a function of the initial energy exhibits a knee-like behaviour, which cannot be reproduced within conventional approaches. The said measurements were performed using liquid ${}^4\text{He}$ [21]; the use of a gas target [22] permitted to measure the invariant mass of the $pp\pi^-$ system. The small statistic and low sensitivity to charged particles with energies below 5–7 MeV, however, reduces the significance of this exclusive measurement.

The most elementary reaction in which d' can be produced via strong interaction is $pp \rightarrow d'\pi^+$. Hence, to search for an NN -decoupled resonance in proton-proton collisions one has to investigate, for example, the two-pion production, $pp \rightarrow pp\pi^-\pi^+$, and to look for the d' -signal in the invariant-mass spectrum $M_{pp\pi^-}$.

The first exclusive measurements of two-pion production in NN -collisions [24] at $T_p = 750$ MeV revealed a narrow peak at $M_{pp\pi^-} \approx 2.06$ GeV. The authors of ref. [25] also reported evidence of a resonance-like structure in the $pp\pi^-$ invariant-mass spectrum. However, subsequent experiments with higher statistics did not corroborate these findings [26].

The only reaction where d' can be produced in the s -channel is $\gamma d \rightarrow d' \rightarrow NN\pi$. In the range of $2.02 < M_{pp\pi^-} < 2.1$ GeV no narrow structures have been found with upper limits within a few microbarns [27]. However, this limit is still an order of magnitude above the expectation for d' production.

An intriguing possibility to look for the d' would be pion electroproduction off the deuteron at a large momentum transfer. At present, however, there are no data which could be conclusive for the $NN\pi$ -resonance with a mass of about 50 MeV above the threshold.

From all available experimental results of d' searches one can conclude that no unambiguous answer to the question concerning the d' existence has been found yet.

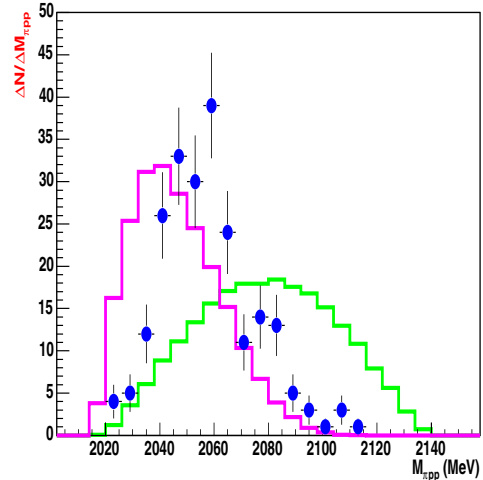


Fig. 3. $pp\pi^-$ invariant-mass distribution. The measured spectrum is shown by dots with error bars. Right and left histograms are results of MC simulations for DCX transitions $\pi^+ + {}^{107}\text{Ag} \rightarrow {}^{105}\text{Ag} + pp\pi^-$ and $\pi^+ + {}^{107}\text{Ag} \rightarrow {}^{103}\text{Ag} + pp\pi^- + 2n$, respectively.

4 Analysis of the $pp\pi^-$ invariant-mass spectrum

In this section we present the measured distribution of $M_{pp\pi^-}$, and analyse possible reaction channels of the pionic double charge exchange on nuclear photoemulsion accompanied by the emission of two protons.

As it was already explained in sect. 2, the reaction mainly takes place on heavy isotopes (Ag and Br). Thus, for example, in the case of Ag isotopes, the following reactions can contribute to the double charge exchange, in which final states contain only stable isotopes:

$$\pi^+ + {}^{107}\text{Ag} \rightarrow {}^{105}\text{Ag} + pp\pi^-, \quad (4)$$

$$\pi^+ + {}^{109}\text{Ag} \rightarrow {}^{107}\text{Ag} + pp\pi^-, \quad (5)$$

$$\pi^+ + {}^{109}\text{Ag} \rightarrow {}^{105}\text{Ag} + pp\pi^- + 2n, \quad (6)$$

$$\pi^+ + {}^{107}\text{Ag} \rightarrow {}^{103}\text{Ag} + pp\pi^- + 2n, \quad (7)$$

$$\pi^+ + {}^{107}\text{Ag} \rightarrow {}^{54}\text{Cr} + {}^{51}\text{V} + pp\pi^-. \quad (8)$$

Similar reactions can take place on Br isotopes:

$$\pi^+ + {}^{81}\text{Br} \rightarrow {}^{79}\text{Br} + pp\pi^-, \quad (9)$$

$$\pi^+ + {}^{81}\text{Br} \rightarrow {}^{77}\text{Br} + pp\pi^- + 2n, \quad (10)$$

$$\pi^+ + {}^{79}\text{Br} \rightarrow {}^{77}\text{Br} + pp\pi^-, \quad (11)$$

$$\pi^+ + {}^{79}\text{Br} \rightarrow {}^{37}\text{Cl} + {}^{40}\text{Ar} + pp\pi^-. \quad (12)$$

All other reactions on Ag and Br isotopes induced by π^+ (with the $pp\pi^-$ subsystem in the exit channel) produce radioactive isotopes and are discarded.

Shown in fig. 3 are experimental data in comparison with $M_{pp\pi^-}$ distributions for reactions (4) and (7) (right and left histograms, respectively).

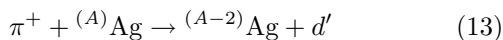
The $pp\pi^-$ invariant-mass distributions for the reactions (5), (9) and (11) do practically not differ from the

distribution for the reaction (4). The histograms for reactions with extra two neutrons (6), (7) and (10) are also very close to each other. The distribution over $M_{pp\pi^-}$ for the cases when production of the $pp\pi^-$ subsystem is accompanied by a breakup of the rest of the nucleus (reactions (8) and (12)) appears to be very similar to the $M_{pp\pi^-}$ spectrum for reactions (4), (5), (9) and (11), which is not surprising, because the energy carried away by heavy fragments is negligible.

This is the reason to present in fig. 3 two kinds of MC simulations for those reactions, in which the $M_{pp\pi^-}$ spectra are essentially different. The histograms shown in fig. 3 represent phase space distributions for the reactions listed above. As can be seen, none of them (neither their combination) can satisfactorily reproduce the observed $M_{pp\pi^-}$ spectrum. The experimental resolution for the $M_{pp\pi^-}$ invariant-mass distribution is ~ 10 MeV; it has been taken into account in our simulations shown in fig. 3.

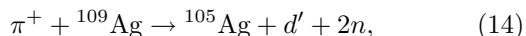
Taking into account NN FSI (see sect. 5) does not allow to achieve agreement between the simulated results and experimental data. Inclusion of the pp FSI shifts the left histogram to the region of even smaller values of $M_{pp\pi^-}$, while nn FSI practically leaves the shape of the left histogram and the position of its maximum practically intact. As for the right histogram, it stays as wide as in fig. 3 after taking into consideration NN FSI.

Another possibility could be the production of the $pp\pi^-$ system via the d' -resonance,



with subsequent decay of d' into $pp\pi^-$. A similar production of d' can, of course, take place on Br isotopes.

The resonance mechanism should also contribute to the production of the $pp\pi^-$ system when produced together with two extra neutrons:



which is the resonance mechanism of reactions (6) and (7). If d' really exists, its effect in the $pp\pi^-$ invariant-mass spectrum should be similar for reactions (13) and (14). Threshold energies for the production of d' in reactions (13) for $A = 109$ and 107 , and in reaction (14) are different and are readily calculated. This was automatically taken into consideration when the $M_{pp\pi^-}$ distributions were averaged over the spectrum of the incident π^+ -mesons, which is nearly flat. This averaging takes into account that for any particular value of $M_{pp\pi^-}$ there is a certain (minimal) value of energy of the incident π^+ .

A similar procedure for averaging the $M_{pp\pi^-}$ spectrum was also performed for the non-resonant mechanisms discussed above (fig. 3). The resonance contribution is shown in fig. 4.

As can be seen, the resonance contribution provides a reasonable fit of the experimentally observed $pp\pi^-$ invariant-mass distribution. The mass of the resonance required for the description of the experimental $M_{pp\pi^-}$ spectrum is almost equal to 2.05 GeV. This value practically coincides with the one deduced from the pionic DCX described in sect. 3. The width of the resonance, fitted from

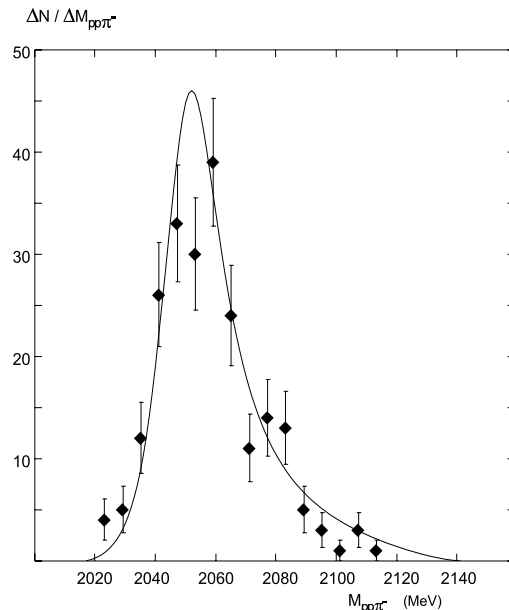


Fig. 4. Resonant description of $pp\pi^-$ invariant-mass spectrum in comparison with experimental data for the reaction $\pi^+ + {}^{107}\text{Ag} \rightarrow {}^{105}\text{Ag} + pp\pi^-$.

the experimental data shown in fig. 4, is about 20 MeV. It deserves mentioning that the vacuum width of d' deduced from the data on DCX transitions to the discrete levels is only $1/2$ – 1 MeV, while its total width in a nuclear medium was found to be 15 – 20 MeV. In the reaction under consideration there must also be nuclear-medium effects, and hence the observed width of the resonance must be closer to its width in a nuclear medium than to its vacuum width. Thus, the parameters of the resonance required for fitting the $M_{pp\pi^-}$ spectrum coincide with the corresponding parameters deduced from DCX transitions to discrete levels. It must be mentioned that the fitted width of the resonance is to be understood as an effective width, which takes into account the vacuum width, the width of the resonance in nuclear medium and the broadening of the $M_{pp\pi^-}$ distribution due to the experimental resolution. Thus the physical width (which is mainly governed by nuclear-medium effects) is somewhat smaller than the one used to calculate the resonant contribution (solid curve in fig. 4).

5 pp final-state interaction

An effective way to study more about the reaction mechanism of $pp\pi^-$ production in the double charge exchange reaction is to investigate the pp invariant-mass distribution. As is well known, the low-mass side of the M_{pp} spectrum must be affected by the Migdal-Watson effect of the NN final-state interaction (FSI) [28, 29] when the two nucleons are in a relative s -wave. The enhancement factor of the M_{pp} spectrum can be calculated from

$$F = |1 + A|^2 F_C(pa_c), \quad (15)$$

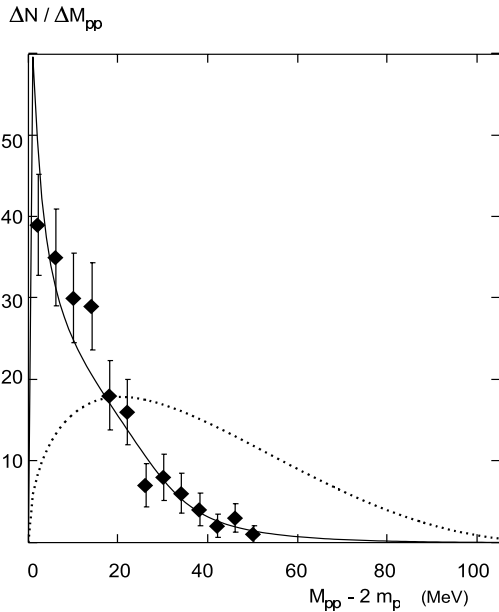


Fig. 5. pp invariant-mass distribution in the reaction $\pi^+ + {}^{107}\text{Ag} \rightarrow {}^{105}\text{Ag} + pp \pi^-$: experimental points and fit of the data are based on eq. (15). The dotted curve is the phase space distribution for the reaction $\pi^+ + {}^{107}\text{Ag} \rightarrow {}^{105}\text{Ag} + pp \pi^-$.

$$A = \frac{\rho^{-1}}{-a_s^{-1} + \frac{1}{2}r_0p^2 - \frac{2}{a_c}h(pa_c) - ipF_C(pa_c)}.$$

Here $a_s = -7.8$ fm is the pp scattering length, $r_0 = 2.8$ fm is the effective range, p is the momentum of either proton in their c.o.m., $p = \sqrt{M_{pp}^2/4 - m_p^2}$;

$$F_C(x) = \frac{2\pi/x}{e^{2\pi/x} - 1}, \quad (16)$$

$$h(x) = \frac{1}{x^2} \sum_{n=1}^{\infty} \frac{1}{n(n^2 + x^{-2})} - \gamma + \ln(x), \quad (17)$$

$\gamma \approx 0.577$ is the Euler constant, and $a_c = 57.5$ fm.

The formula for calculation of the FSI effect takes into account Coulomb repulsion. The enhancement factor given by eq. (15) contains a sole parameter ρ , the value of which depends on the particular reaction mechanism. The smaller the interaction region, in which the two nucleons are produced, the smaller the parameter ρ , and the stronger the effect of NN FSI. Thus, for example, if the two-proton source is considered pointlike, the parameter ρ can be as small as ~ 1 fm. This estimate can be found from the Yamaguchi model for the NN wave function in the continuum [30].

Shown in fig. 5 is the pp invariant-mass distribution. Experimental data demonstrate a rather strong enhancement of the low-mass side of the M_{pp} spectrum. This may point to significant pp FSI if the DCX transition is dominated by the reaction mechanism without emission of two neutrons.

The dotted curve is the phase space distribution of M_{pp} for reaction (4). The solid curve takes into consideration

pp FSI calculated using eq. (15). The parameter ρ needed to describe the observed FSI effect was found to be $\rho = 1.1$ fm.

Such a strong FSI effect can hardly be expected for conventional (non-resonant) production of the $pp\pi^-$ system.

At the same time, it is quite reasonable for the resonant production of the $pp\pi^-$ system if d' is basically a $6q$ -object with a typical hadronic size ~ 1 – 1.5 fm.

6 Conclusion

Two hundred and twenty-four positive-pion DCX events on heavy nuclei in photoemulsion have been analysed and the invariant $M_{pp\pi^-}$ spectrum has been shown to indicate a resonant behaviour at low energies.

We are grateful to I. Gnesi for help. This work was partially supported by the grant SH-2328.2003.2 and by the RFBR grant 05-02-17471.

References

1. R. Bilger, H. Clement, M. Schepkin, Phys. Rev. Lett. **71**, 42 (1993).
2. R. Bilger, H. Clement, K. Foehl, K. Heitlinger, C. Joram, W. Kluge, M. Schepkin, G.J. Wagner, R. Wieser, R. Abela, F. Foroughi, D. Renker, Z. Phys. A **343**, 491 (1992).
3. B. Martemyanov, M. Schepkin, JETP Lett. **53**, 139 (1991).
4. Yu.A. Batusov, S.A. Bunyatov, V.M. Sidorov, V.A. Yarba, JETP **46**, 817 (1964) (in Russian).
5. Yu.A. Batusov, S.A. Bunyatov, V.M. Sidorov, V.A. Yarba, Sov. J. Nucl. Phys. **1**, 271 (1965).
6. Yu.A. Batusov, S.A. Bunyatov, V.M. Sidorov, V.A. Yarba, Sov. J. Nucl. Phys. **3**, 223 (1966).
7. Yu.A. Batusov, S.A. Bunyatov, V.M. Sidorov, V.A. Yarba, Yad. Fiz. **6**, 998 (1967) (in Russian).
8. Yu.A. Batusov, V.I. Kochkin, V.M. Malzev, Yad. Fiz. **6**, 158 (1967) (in Russian).
9. R. Kalpakchieva, Yu.E. Penionzhkevich, H.G. Bohlen, Phys. Part. Nucl. **29**, 341 (1998).
10. N. Auerbach, W.R. Gibbs, Joseph N. Ginocchio, W.B. Kaufmann, Phys. Rev. C **38**, 1277 (1988).
11. H. Clement, Prog. Part. Nucl. Phys. **29**, 175 (1992).
12. J. Draeger, R. Bilger, H. Clement, M. Cröni, H. Denz, J. Gräter, R. Meier, J. Pätzold, D. Schapler, G.J. Wagner, O. Wilhelm, K. Föhl, M. Schepkin, Phys. Rev. C **62**, 064615 (2000).
13. K. Foehl, R. Bilger, H. Clement, J. Gräter, R. Meier, J. Pätzold, D. Schapler, G.J. Wagner, O. Wilhelm, W. Kluge, R. Wieser, M. Schepkin, R. Abela, F. Foroughi, D. Renker, Phys. Rev. Lett. **79**, 3849 (1997).
14. A.V. Nefediev, M.G. Schepkin, H.A. Clement, Phys. Rev. C **67**, 015201 (2003).
15. R. Gilman, H.T. Fortune, M.B. Johnson, E.R. Siciliano, H. Toki, A. Wirzba, B.A. Brown, Phys. Rev. C **34**, 1895 (1986).

16. R. Gilman, H.T. Fortune, J.D. Zumbro, C.M. Laymon, G.R. Bureson, J.A. Faucett, W.B. Cottingham, C.L. Morris Peter A. Seidl, C. Fred Moore, L.C. Bland, Rex R. Kiziah S. Mordechai, Kalvir S. Dhuga, *Phys. Rev. C* **35**, 1334 (1987).
17. M. Nuseirat, M.A.K. Lodhi, M.O. El-Ghossain, W.R. Gibbs, W.B. Kaufmann, *Phys. Rev. C* **58**, 2292 (1998).
18. H.C. Wu, W.R. Gibbs, *Phys. Rev. C* **62**, 044614 (2000).
19. I.V. Falomkin, M.M. Kulyukin, V.I. Lyashenko, G.B. Pontecorvo, Yu.A. Shcherbakov, C. Georgescu, A. Mihul, F. Nichitiu, A. Seraru, G. Piragino, *Nuovo Cimento A* **22**, 333 (1974).
20. I.V. Falomkin, V.I. Lyashenko, G.B. Pontecorvo, Yu.A. Shcherbakov, M. Albu, A. Mihul, F. Nichitiu, A. Seraru, F. Balestra, R. Garfagnini, G. Piragino, *Lett. Nuovo Cimento* **16**, 525 (1976).
21. J. Gräter, R. Bilger, H. Clement, R. Meier, G.J. Wagner, E. Friedman, M. Schepkin, P.A. Amaudruz, L. Felawka, D. Ottewell, G.R. Smith, A. Ambardar, G.J. Hofman, M. Kermani, G. Tagliente, F. Bonutti, P. Camerini, N. Grion, R. Rui, P. Hong, E.L. Mathie, R. Tacik, J. Clark, M.E. Sevier, O. Patarakin, *Phys. Rev. C* **58**, 1576 (1998).
22. J.L. Clark, M.E. Sevier, H. Clement, J. Gräter, R. Meier, G.J. Wagner, P.-A. Amaudruz, L. Felawka, G.J. Hofman, D. Ottewell, G.R. Smith, A. Ambardar, M. Kermani, G. Tagliente, P. Camerini, E. Fragiaco, N. Grion, R. Rui, E.L. Mathie, R. Tacik, D.M. Yeomans, E.F. Gibson, J.T. Brack, M. Schepkin, *Phys. Rev. C* **66**, 054606 (2002).
23. J. Gräter, R. Bilger, H. Clement, R. Meier, J. Pätzold, G.J. Wagner, E. Friedman, E.L. Mathie, R. Tacik, M. Yeomans, P.A. Amaudruz, L. Felawka, D. Ottewell, K. Raywood, G.R. Smith, G.J. Hofman, B. Jamieson, M. Kermani, G. Tagliente, P. Camerini, E. Fragiaco, N. Grion, R. Riu, J. Clark, G. Moloney, M.E. Sevier, A. Nefediev, M. Schepkin, E.F. Gibson, O. Patarakin, H. Staudenmaier, S.N. Filipov, Yu.K. Gavrilov, T.L. Karavicheva, *Phys. Lett. B* **471**, 113 (1999).
24. W. Brodowski, R. Bilger, H. Calen, H. Clement, C. Ekstroem, K. Foehl, K. Fransson, L. Gustafsson, S. Haegstroem, B. Hoistad, A. Johansson, T. Johansson, K. Kilian, S. Kullander, A. Kupsc, G. Kurz, P. Marciniowski, B. Morosov, J. Moehn, A. Moertsell, W. Oelert, V. Renken, R. Ruber, M.G. Schepkin, U. Siodlaczek, J. Stepaniak, A. Sukhanov, A. Turowiecki, G.J. Wagner, Z. Wilhelmi, J. Zabierowski, A. Zernov, J. Zlomanczuk, *Z. Phys. A* **355**, 5 (1996).
25. L.S. Vorobyev, Yu.G. Grishuk, Yu.V. Efremenko, M.V. Kossov, S.V. Kuleshov, G.A. Leksin, N.A. Pivnyuk, A.V. Smirnitsky, V.B. Fedorov, B.B. Shvartzman, S.M. Shvalov, M.G. Schepkin, *Phys. At. Nucl.* **61**, 771 (1998); *JEPT Lett.* **59**, 77 (1994).
26. W. Brodowski, J. Pätzold, R. Bilger, H. Calen, C. Ekström, K. Fransson, J. Greiff, S. Haggstrom, B. Hoistad, J. Johanson, A. Johansson, T. Johansson, K. Kilian, S. Kullander, A. Kupsc, P. Marciniowski, B. Morosov, W. Oelert, R.J.M.Y. Ruber, M. Schepkin, W. Scobel, J. Stepaniak, A. Sukhanov, A. Turowiecki, G.J. Wagner, Z. Wilhelmi, J. Zabierowski, J. Zlomanczuk, *Phys. Lett. B* **550**, 147 (2002).
27. U. Siodlaczek, P. Achenbach, J. Ahrens, H.J. Arends, R. Beck, R. Bilger, H. Clement, V. Hejny, J.D. Kellie, M. Kotulla, B. Krusche, V. Kuhr, R. Leukel, J.C. McGeorge, V. Metag, R. Novotny, V. Olmos de Leon, F. Rambo, M. Schepkin, A. Schmidt, H. Stroher, G.J. Wagner, T. Walcher, J. Weiss, F. Wissmann, M. Wolf, *Eur. Phys. J. A* **9**, 309 (2000).
28. K.M. Watson, *Phys. Rev.* **88**, 1163 (1952).
29. A.B. Migdal, *Sov. Phys. JETP* **1**, 2 (1955).
30. Y. Yamaguchi, *Phys. Rev.* **95**, 1628 (1954).